Systemic injury caused by taurocholate-induced severe acute pancreatitis in rats

XIN-XIN HONG[1*], HONG-YAN WANG[1*], JIONG-MING YANG[2], BAO-FU LIN[1], QIN-QIN MIN[1], YI-ZHONG LIANG[1], PEI-DI HUANG[1], ZI-YOU ZHONG[1], SHAO-JU GUO[1], BIN HUANG[1] and YI-FEI XU[1]

[1]Shenzhen Traditional Chinese Medicine Hospital, The Fourth Clinical Medical College of Guangzhou University of Chinese Medicine, Shenzhen, Guangdong 518033; [2]School of Pharmaceutical Sciences, Guangzhou University of Chinese Medicine, Guangzhou, Guangdong 510006, P.R. China

Received February 11, 2022; Accepted May 13, 2022

DOI: 10.3892/etm.2022.11395

Abstract. Systemic injury plays a central role in severe acute pancreatitis (SAP). Retrograde biliopancreatic duct infusion of sodium taurocholate (NaT) is commonly used to establish SAP animal models. To better characterize the systemic injury in this model, SAP was induced in Sprague-Dawley rats by NaT administration (3.5 or 5%), followed by sacrifice at 3, 6, 9, 12, 24, 48 and 72 h. Normal saline was used as a control in Sham-operated rats. The mortality rate, ascites volume, and serum and ascitic fluid amylase and lipase activities were assessed. Multiple organ dysfunction, including dysfunction of the pancreas, lung, ileum, liver, and kidney, was investigated using hematoxylin and eosin staining. The interleukin (IL)-1β, IL-6, and tumor necrosis factor-α levels in the ascitic fluid, serum, and ileum tissues were evaluated using an enzyme-linked immunosorbent assay (ELISA). Tight junction proteins, zonula occludens-1 (ZO-1) and occludin, in ileum tissues were studied using immunofluorescence. Aspartate aminotransferase (AST), alanine aminotransferase (ALT), creatinine (CRE) and urea levels were measured using an automatic biochemical analyzer. The results of the present study indicated that both 3.5 and 5% NaT could induce a stable elevation of pancreatitis indices, with histopathological injury of the pancreas, lungs and ileum (5% NaT). The ascitic fluid levels of IL-6 and IL-1β were increased in the 5% NaT group. ALT and AST levels increased temporarily and recovered in 72 h, without a significant increase in CRE and urea levels or apparent hepatic and renal pathological injury. In conclusion, rats with NaT-induced SAP have characteristics of necrotizing hemorrhagic pancreatitis with multiple organ injuries, including inflammatory lung injury, ischemic intestinal injury and slight liver and kidney injuries.

Correspondence to: Dr Yi-Fei Xu, Shenzhen Traditional Chinese Medicine Hospital, The Fourth Clinical Medical College of Guangzhou University of Chinese Medicine, 1 Fuhua Road, Futian, Shenzhen, Guangdong 518033, P.R. China
E-mail: xyf2995@gzucm.edu.cn

*Contributed equally

Abbreviations: SAP, severe acute pancreatitis; IL, interleukin; TNF, tumor necrosis factor; ELISA, enzyme-linked immunosorbent assay; ZO-1, zonula occludens-1; AST, aspartate aminotransferase; ALT, alanine aminotransferase; CRE, creatinine; NS, normal saline; HE, hematoxylin and eosin; MPO, lung myeloperoxidase; MDA, malondialdehyde

Key words: severe acute pancreatitis, systemic injury, organ failure, rat model, sodium taurocholate

Introduction

Acute pancreatitis (AP) is a potentially lethal disease accompanied by systemic injury, and ~20% of patients develop moderate or severe acute pancreatitis (SAP) (1). According to global estimates, the annual morbidity of AP is ~33.74 cases (95% confidence interval: 23.33-48.81) per 100,000 person-years (2). The mortality rate of SAP may reach 20-40% when accompanied by pancreatic or peripancreatic tissue necrosis or organ failure (3-5). The severity of AP is classified as mild, moderately severe, or severe based on the presence of organ failure and local or systemic complications according to the revised Atlanta classification (6). Although numerous advances have been made in the treatment of AP, there is still a lack of specific and effective drug therapies because the pathophysiology of the disease is poorly understood (7).

Sodium taurocholate (NaT), a natural bile salt, may rapidly and directly impair the surrounding acinar cells in a few minutes (8,9). NaT may also trigger pathological acinar cell calcium transients, cell death and calcium-dependent trypsinogen activation (10,11). Retrograde pancreatic duct infusion of NaT is a common method of inducing AP (10,12). Different extent of the pancreatic injury can be induced by changing the concentration, perfusion rate and volume of NaT (12,13). However, different researchers have redesigned the dosage of NaT and timing for study to meet their own research needs, resulting in difficulties in the application of this model, as well as further efficacy evaluation. Based on previous studies, several NaT concentrations between 3.5 and 6% (1 ml/kg) have been reported to induce SAP in rats (14-17). However, differences in the modeling conditions of rat models

result in poor comparability between different SAP efficacy and mechanism experiments.

Moreover, previous studies have strongly emphasized local rather than systemic pancreatic injury, and systemic organ dysfunction in this animal model remains controversial and unclear. Organ failure is the most critical factor affecting mortality in patients with SAP (18). Early organ dysfunction is attributed to sterile injury and inflammation caused by damage-associated molecular patterns and unsaturated fatty acids (19). Patients with persistent systemic inflammatory response syndrome (SIRS) are prone to developing systemic organ dysfunction and later organ failure due to pathogen-associated molecular patterns (20,21). The lungs, liver, kidneys and heart are often involved in AP-related multiple organ failure (3). Secondary infection with pancreatic or peripancreatic necrosis is considered to be a result of bacterial translocation of intestinal microorganisms (22). Disruption of the tight junction of the intestinal mucosa is a frequent cause of AP-related SIRS and sepsis. Zonula occludens-1 (ZO-1) and occludin are the most extensively used tight junction structural markers. ZO-1 expression is downregulated in AP and inversely correlated with the intensity of inflammation (23).

In the present study, the damage to numerous organs (pancreas, lung, ileum, liver and kidney) and systemic inflammation, induced by retrograde injection of 3.5 or 5% NaT into the rat pancreatic duct, were evaluated.

Materials and methods

Animals. A total of 192 male specific pathogen-free Sprague-Dawley rats (weight, 300±20 g) were purchased from the Experimental Animal Center of Guangzhou University of Chinese Medicine (Guangzhou, China) and housed under standard laboratory conditions (12/12 h light-dark cycle, 21±2˚C, humidity 50±10%) with food and water provided *ad libitum* during the study. All animal procedures were conducted in accordance with the Guidelines for Animal Care of Guangzhou University of Chinese Medicine and were approved (approval no. ZYD-2020-028) by the Animal Care and Use Committee of Guangzhou University of Chinese Medicine (Guangzhou, China). All efforts were made to minimize animal suffering.

NaT-induced pancreatitis. Male Sprague-Dawley rats were divided into the following four groups using the random weight method: i) Sham, ii) normal saline (NS), iii) 3.5% NaT, and iv) 5% NaT. Sham group rats underwent Sham operation and were treated similarly without infusion (n=16), NS group rats were infused with NS solution and underwent Sham operation (n=16), whereas SAP was induced in 3.5% NaT group rats (n=80) (3, 6, 12, 24, 48 and 72 h) and 5% NaT group rats (n=80) (3, 6, 12, 24, 48 and 72 h) according to a previously reported method (13,15,16). Rats were fasted for 12 h before the operation. Anesthesia was induced using isoflurane (RWD Life Science) and an R550 Multi-output Anesthesia Machine (RWD Life Science) before the onset of surgery. Briefly, a midline laparotomy was performed after sterilization, and the duodenum was identified and gently rotated to expose the posterior surface and pancreas. The proximal biliopancreatic duct was then temporarily occluded with a microclip. The cannula was passed through the duodenal wall to the papilla and into the pancreatic duct. Next, 3.5 or 5% NaT (Sigma-Aldrich; Merck KGaA) at 1 ml/kg was infused into the pancreatic duct at a constant rate (6 ml/h) and pressure, using a syringe pump (Leienly Company). After the infusion, the cannula and microclips were removed from the biliopancreatic duct. Finally, the peritoneum and skin were sutured using a 4-0 prolene suture. After surgery, all the rats were administered NS (1 ml/kg) and placed on a heated pad (37˚C) until they recovered. Animals in the Sham and NS groups were euthanized at 72 h, whereas NaT-induced SAP animals were euthanized at 3, 6, 12, 24, 48 and 72 h after overdosage of isoflurane anesthesia (≥5% for >1 min after cessation of breathing stops). Due to the difficulty of surgery and the high mortality rate in this model, particularly in the 5% NaT group, no rats survived in the 5% NaT-72 h group. The rest of the sample distribution was as follows: Sham group (n=16), NS group (n=16), 3.5% NaT-3 h (n=15), 3.5% NaT-6 h (n=15), 3.5% NaT-12 h (n=13), 3.5% NaT-24 h (n=14), 3.5% NaT-48 h (n=5), 3.5% NaT-72 h (n=4), 5% NaT-3 h (n=15), 5% NaT-6 h (n=13), 5% NaT-12 h (n=11), 5% NaT-24 h (n=7), 5% NaT-48 h (n=3), and 5% NaT-72 h (n=none).

Blood was collected from the abdominal aorta, and ascitic fluid was collected under isoflurane anesthesia before euthanasia. All blood and ascitic fluid samples were centrifuged at 1,000 x g, 4˚C for 15 min, and maintained at -80˚C until use. Tissue samples from the pancreas, lung, ileum, liver and kidneys were harvested and fixed in 4% paraformaldehyde (Dalian Meilun Biology Technology Co., Ltd.) at room temperature for over 24 h, embedded in paraffin blocks, or stored at -80˚C until use.

Histopathological analysis. Tissue sections were stained with hematoxylin and eosin (H&E) for histopathological evaluation. After dewaxed and dehydration, tissue sections were stained with hematoxylin at room temperature for 5 min, followed by differentiation and bluing, then stained with eosin at room temperature for 1 min. For each group, the pancreatic histopathological scores of three independent tissue sections were blindly assessed by two pathologists according to the scoring criteria developed by Schmidt *et al* (23) and simplified by Liu *et al* (15). Briefly, the pancreatic histopathological scoring criteria included four aspects: i) interstitial edema: 0 points=none, 1 point=interlobular, 2 points=lobule involvement, and 3 points=isolated island-like acinar cells; ii) leukocyte infiltration: 0 points=none, 1 point=<20%, 2 points=20-50%, and 3 points=>50%; iii) acinar cell necrosis: 0 points=none, 1 point=<5%, 2 points=5-20%, and 3 points=>20%; (iv) hemorrhage: 0 points=none, 1 point=1-2, 2 points=3-5, and 3 points=>20%. Pulmonary histopathological changes were assessed by areas of alveolar septal thickening, leukocyte infiltration, alveolar capillaries dilation and congestion and hemorrhage.

Serum and ascitic fluid amylase levels. The serum and ascitic fluid amylase levels were determined using starch-iodine colorimetry and α-amylase assay kits (Nanjing Jiancheng Bioengineering Institute). Phosphate-buffered saline (PBS) was used to dilute the pancreatitis rat serum and ascites fluid samples. First, 0.1 ml of serum and ascitic fluid samples were added into 0.5 ml 4 g/ml substrate buffer and placed in a water bath with a water temperature of 37˚C for 7.5 min. Then, 0.5 ml

Table I. Pancreatitis histopathological scores.

Groups (n=3)	Score				
	Interstitial edema	Leukocyte infiltration	Acinar cell necrosis	Hemorrhage	Total
Sham	0.00±0.00	0.00±0.00	0.00±0.00	0.00±0.00	0.00±0.00
NS	0.33±0.33	0.00±0.00	0.00±0.00	0.00±0.00	0.33±0.33
3.5% NaT					
3 h	1.33±0.33	0.00±0.00	1.00±0.00	0.00±0.00	2.33±0.33
6 h	2.33±0.67[b]	0.00±0.00	0.67±0.33	0.00±0.00	3.00±0.58
12 h	2.00±0.58[b]	0.67±0.67	3.00±0.00[b]	2.17±0.44[b]	7.83±1.30[b]
24 h	2.00±0.00[b]	0.67±0.33	2.00±0.58[b]	1.83±0.44[a]	6.50±1.04[b]
48 h	1.83±0.16[a]	0.83±0.44	2.67±0.17[b]	1.83±0.60[a]	7.17±1.20[b]
72 h	2.00±0.00[b]	1.67±0.33[b]	3.00±0.00[b]	3.00±0.00[b]	9.67±0.33[b]
5% NaT					
3 h	1.00±0.00	0.67±0.17	1.50±0.29[a]	1.17±0.73	4.33±0.93[b]
6 h	1.33±0.33	1.00±0.00	2.67±0.33[b]	1.00±0.58	6.00±0.00[b]
12 h	1.00±0.00	1.00±0.00	2.67±0.33[b]	2.67±0.33[b]	7.33±0.33[b]
24 h	1.33±0.33	1.17±0.17[a]	3.00±0.00[b]	2.67±0.33[b]	8.17±0.44[b]
48 h	2.50±0.00[b]	1.67±0.17[b]	3.00±0.00[b]	2.33±0.17[b]	9.50±0.00[b]

[a]P<0.05 and [b]P<0.01 vs. NS group. NaT, sodium taurocholate.

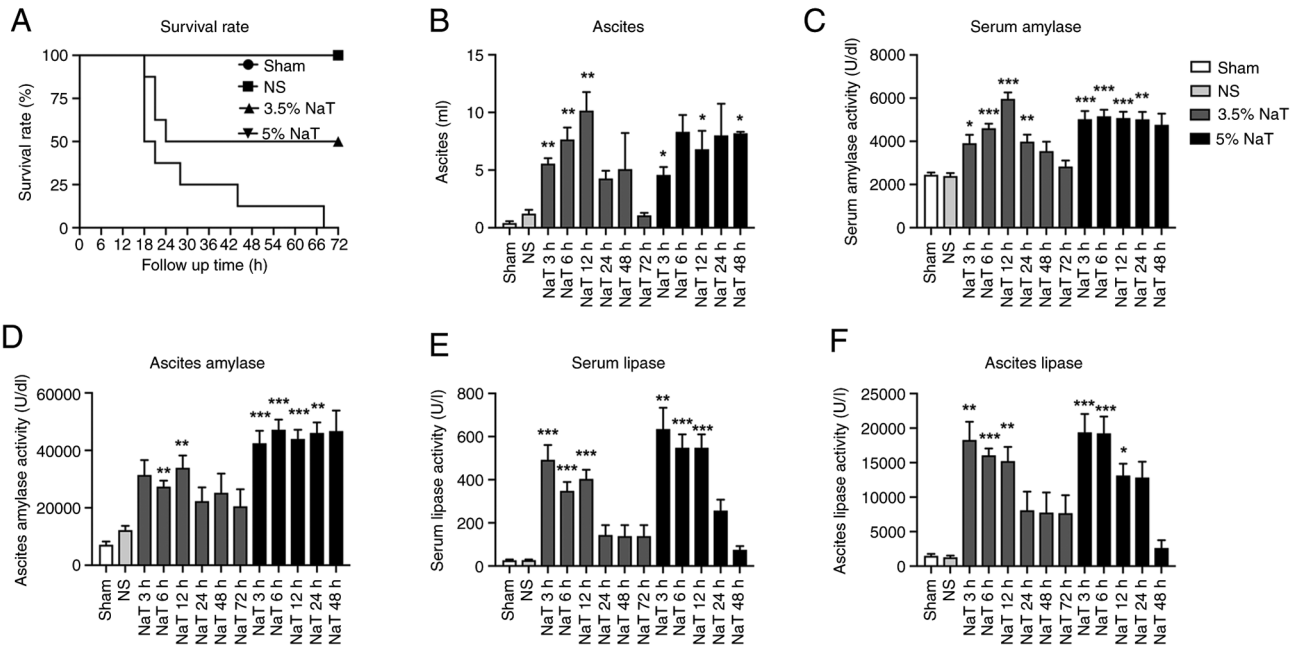

Figure 1. General condition (mortality, ascites volume, and amylase and lipase activities in the serum and ascitic fluid) of rats with NaT-induced SAP. (A) The survival rate of rats with SAP was measured at 72 h. (B) The ascites volume of SAP rats was collected and measured at different time points. (C and D) The amylase activity in the (C) serum and (D) ascitic fluid significantly increased. (E and F) The lipase activity in the (E) serum and (F) ascitic fluid also increased at 3 h. Data are expressed as the mean ± standard error of mean. *P<0.05, **P<0.01 and ***P<0.001 vs. the NS group (n=3-16). Only three rats survived in the 5% NaT groups at 48 h, and no rat survived in the 5% NaT group at 72 h. NaT, sodium taurocholate; SAP, severe acute pancreatitis; NS, normal saline.

0.1 mol/l iodine solution and 3 ml distilled water were added. The absorbance was immediately detected at 660 nm on a UV spectrophotometer (Shanghai Metash Instrument Co., Ltd.).

Serum and ascitic fluid lipase levels. The serum and ascitic fluid lipase levels were determined after dilution (1:1 and 1:10) with PBS using a routine colorimetric method and a lipase assay kit (Nanjing Jiancheng Bioengineering Institute). The substrate buffer was preheated at 37˚C and added to 50 μl fresh serum or ascitic fluid, and the absorbance was detected at 420 nm in the first 30 sec as A1. After 10 min of reaction, the absorbance (A2) was read using a UV spectrophotometer. The

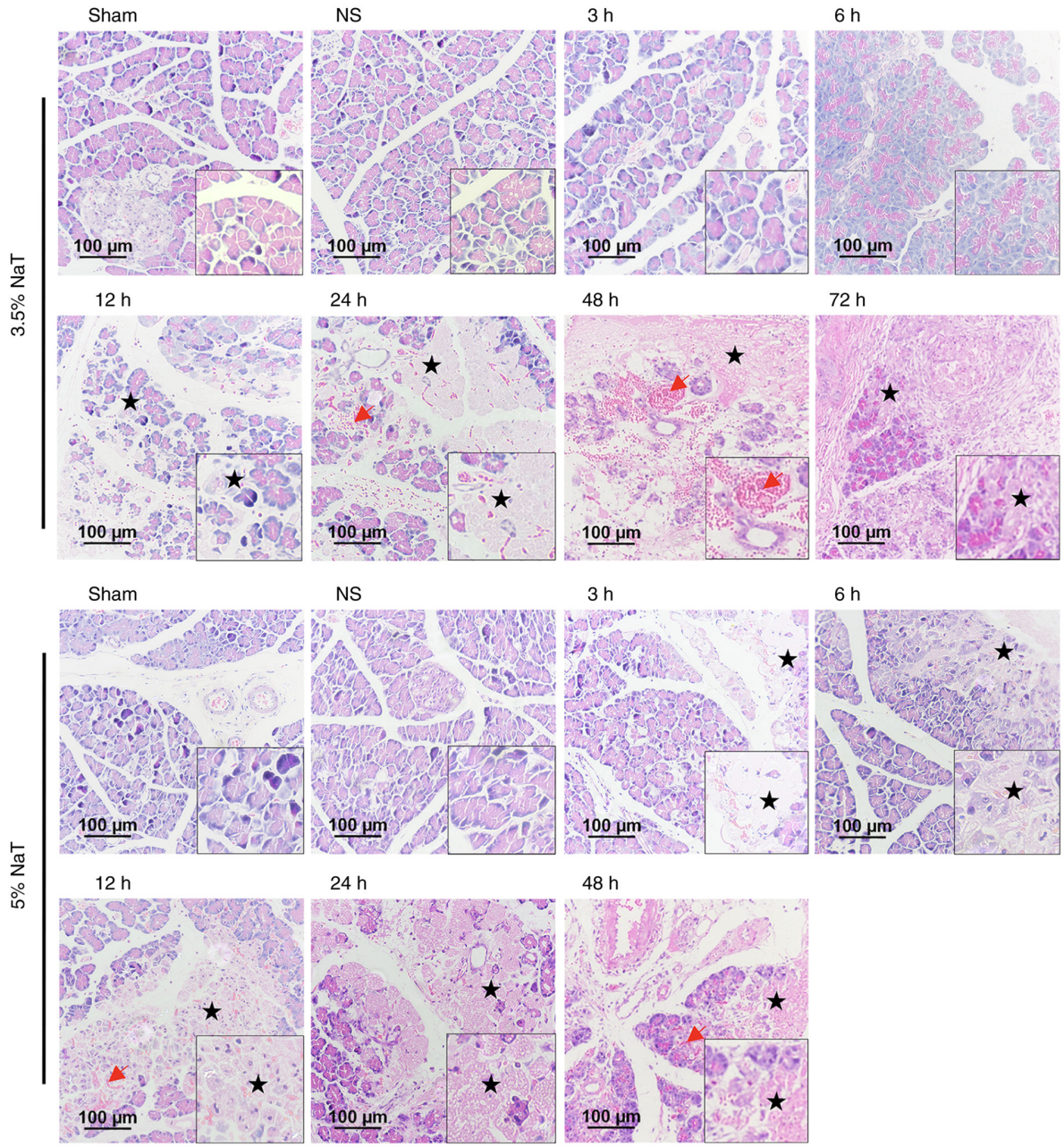

Figure 2. Histopathological changes of the pancreas in NaT-induced severe acute pancreatitis rats. Representative images of hematoxylin and eosin-stained pancreatic sections (magnification, x200; scale bar: 100 μm). Normal pancreatic histology in the Sham and NS groups. In the 3.5% NaT groups, interstitial edema occurred at 3 h and extended at 6 h after pancreatitis induction. Extensive acinar cell necrosis (star) was observed at 12, 24, 48 and 72 h after surgery, with hemorrhage (red arrow). In the 5% NaT groups, the typical pathological features at 3 h were edema and small areas of acinar cell necrosis. Hemorrhage was observed at 6 h, which was exacerbated at 12, 24, and 48 h with severe necrosis. NaT, sodium taurocholate; NS, normal saline.

lipase activity was measured according to the manufacturer's protocol.

Enzyme-linked immunosorbent assay (ELISA). The ileum tissues were lysed in normal saline containing a protease inhibitor. Tissues were ground using an automatic tissue lyser (Jingxin Industrial Development Co., Ltd.). The lysate was collected and centrifuged at 1,000 x g and 4˚C for 15 min. The protein concentration was measured using a BCA Protein Assay Kit (Beyotime Institute of Biotechnology). All samples were stored at -80˚C until use. Enzymatic immunoassays for IL-1β, IL-6, and TNF-α were performed using ELISA kits (cat. nos. CRE0006, CRE0005 and CRE0003; Beijing 4A Biotech Co., Ltd.) according to the manufacturer's protocol. The standard, serum, and ascitic fluid samples were added into a 96-well plate (100 μl/well), which was precoated with IL-1β, IL-6, and TNF-α, respectively. Then, they were incubated at 37˚C for 2 h and washed five times with washing buffer. The corresponding biotinylated antibodies (IL-1β 1:100, IL-6 1:100 and TNF-α 1:100), enzyme-binding antibodies, and tetramethylbenzidine solution were added. Finally, 100 μl stop solution was added to stop the reaction. The absorbance was detected at 450 nm using MULTISKAN GO (Thermo Fisher Scientific, Inc.), the concentrations of each sample were calculated according to the standard curve, and protein concentrations were normalized to tissue cytokine levels.

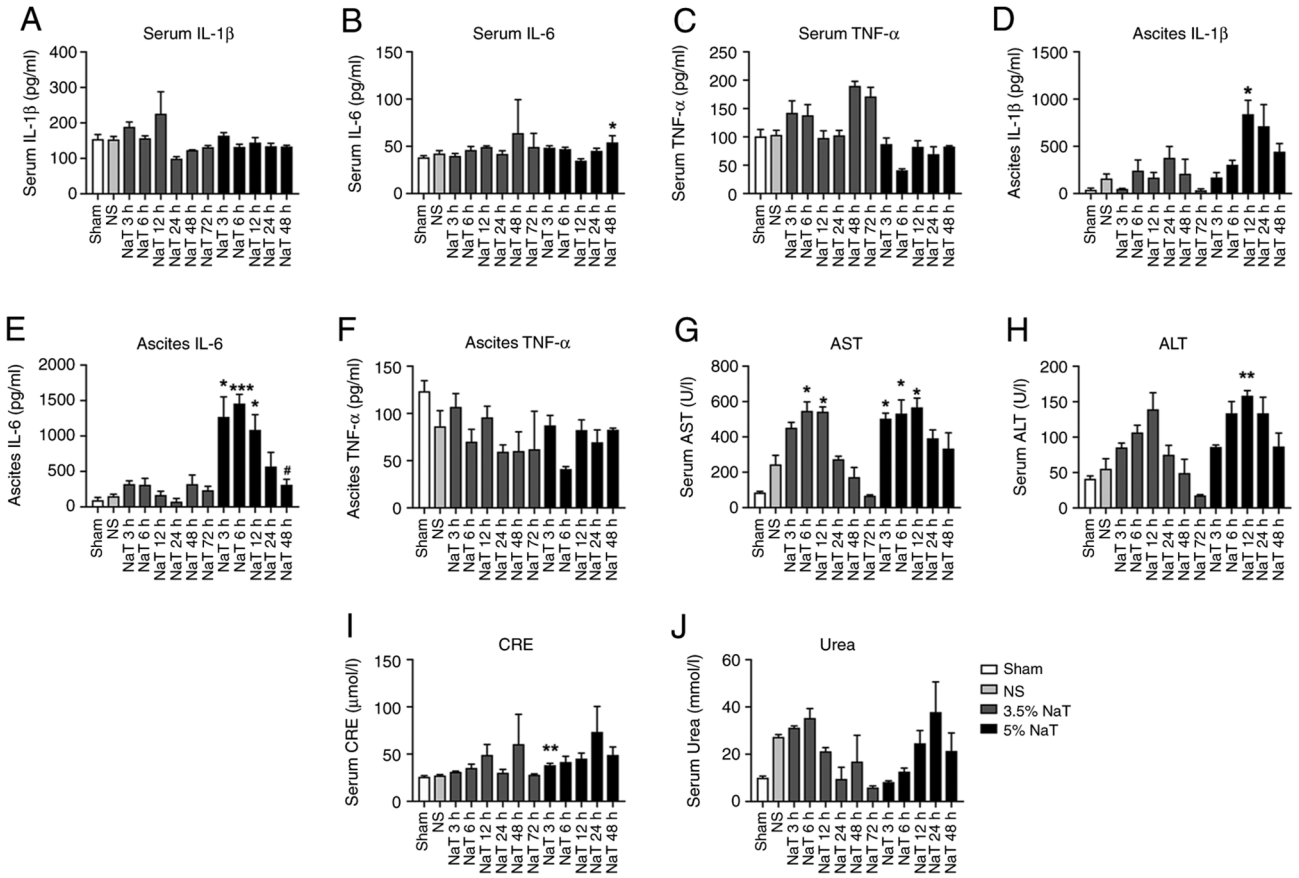

Figure 3. The levels of proinflammatory cytokines, liver function and renal function in NaT-induced severe acute pancreatitis rats. The serum levels of (A) IL-1β, (B) IL-6 and (C) TNF-α, respectively. The ascitic fluid levels of (D) IL-1β, (E) IL-6 and (F) TNF-α, respectively. The serum levels of (G) AST, (H) ALT, (I) CRE, and (J) Urea, respectively. Data are expressed as the mean ± standard error of the mean. *P<0.05, **P<0.01 and ***P<0.001 vs. the NS group; $^{\#}$P<0.05 vs. the 5% NaT-12 h group, (n=3-16). NaT, sodium taurocholate; ALT, alanine transaminase; AST, aspartate aminotransferase; CRE, creatinine; NS, normal saline.

Immunofluorescence. Ileum tissue was embedded in an Optimum Cutting Temperature embedding agent, sliced into 10-μm thick sections, and fixed with 4% paraformaldehyde at 4˚C for 30 min. Next, the tissue sections were incubated with 100 μl of 5% donkey serum blocker solution at room temperature for 2 h to block non-specific antigens. A diluted antibody-containing 5% donkey serum PBST (0.05% Tween-20) was prepared of ZO-1 (1:50; cat. no. sc-33725, Santa Cruz Biotechnology, Inc.) or occludin (1:50; cat. no. sc-133256, Santa Cruz Biotechnology, Inc.). Next, 50 μl of the diluted antibody solution was added to each sample and incubated overnight at 4˚C. After washing with PBST for 10 min thrice, the samples were incubated with a PBST-diluted AF488-conjugated secondary antibody (1:200; cat. no. 1010-30, Southern Biotech) for 2 h at room temperature. Then, they were washed with PBST thrice for 10 min each, and stained with Hoechst 33342 (1:1,000; cat. no. 561908, BD Pharmingen) at room temperature for 30 min. An LSM 8000 laser confocal microscope (Carl Zeiss AG) equipped with a camera was used to observe the stained tissue samples and to obtain images.

Biochemical assay. Serum alanine transaminase (ALT), aspartate transaminase (AST), creatinine (CRE), and urea levels were measured using a Hitachi 7080 automatic biochemical analyzer (Hitachi, Ltd.). Lung myeloperoxidase (MPO) levels were determined using MPO ELISA kits (cat. no. CSB-E13689Rb, Cusabio Technology LLC) and malondialdehyde (MDA) activity was determined using the Lipid Peroxidation MDA Assay kit (cat. no. S0131S, Beyotime Institute of Biotechnology) according to the manufacturer's protocol.

Statistical analysis. All data were analyzed using the SPSS software (version 25.0; IBM Corp.) and are presented as the mean ± standard error. After the homogeneity of variance test, one-way ANOVA followed by the least significant difference (LSD) or Games-Howell test was performed for multiple group comparisons. Data were displayed using GraphPad Prism (version 7.0; GraphPad Software, Inc.). P<0.05 was considered to indicate a statistically significant difference.

Results

General condition (mortality, ascites volume, and amylase and lipase activities in the serum and ascitic fluid) of the rats with NaT-induced SAP. SAP rat serum and ascitic fluid were collected at different time points (3, 6, 12, 24, 48 and 72 h) and the amylase and lipase levels were detected. As revealed in Fig. 1A, the mortality rate in the 3.5% NaT-72 h group was ~50%, and most animals succumbed within 24 h. The

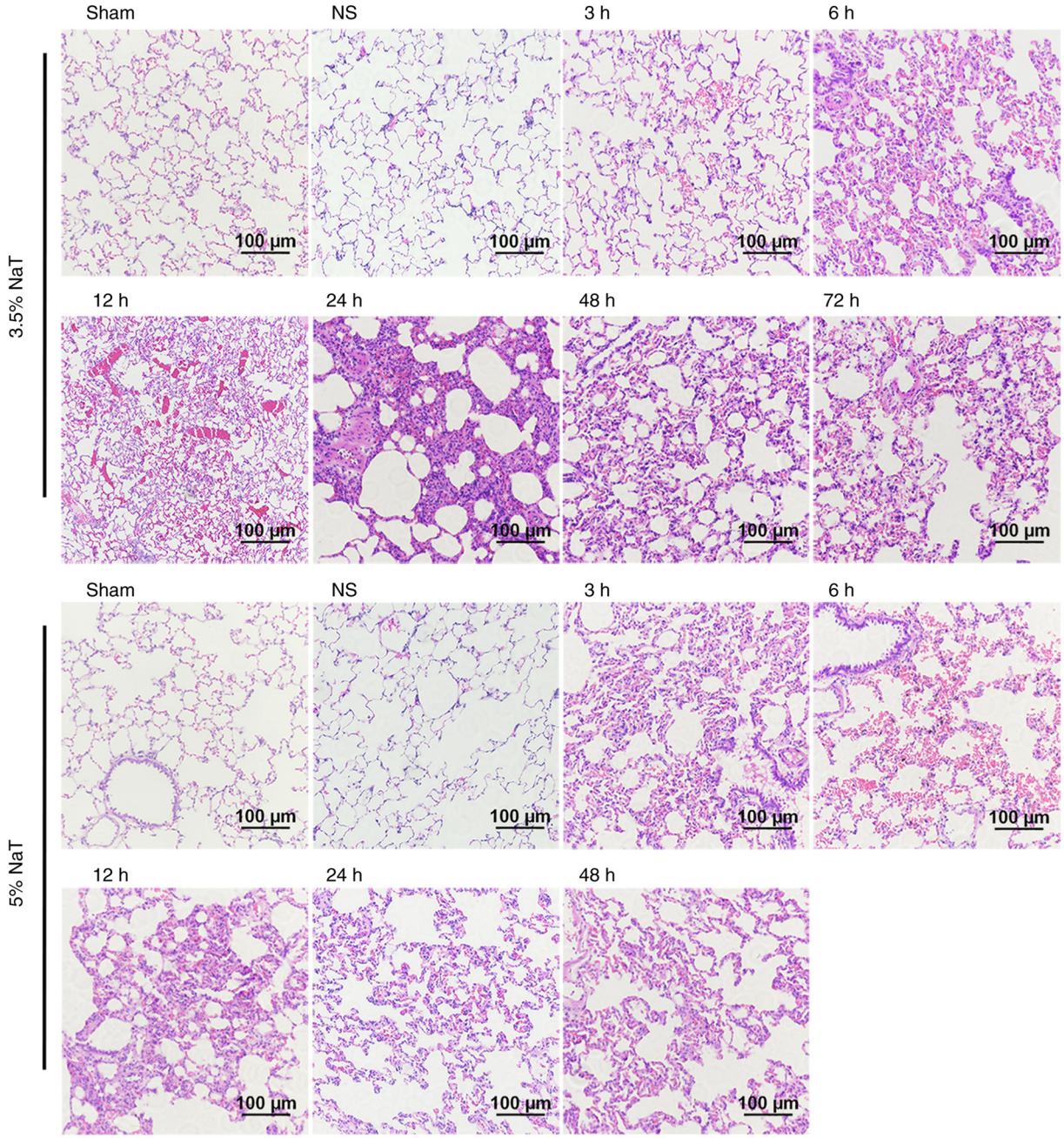

Figure 4. Histopathological changes of the lung in NaT-induced severe acute pancreatitis rats. Representative images of hematoxylin and eosin-stained lung sections (magnification, x200; scale bar: 100 μm). Normal lung histology in the Sham and NS groups. Alveolar septum thickening with partial alveolar collapse was widely observed after surgery in both 3.5 and 5% NaT groups. NaT, sodium taurocholate; NS, normal saline.

mortality rate in the 5% NaT-72 h group was ~100%; therefore, a sample from this group was unobtainable.

The ascites volume increased 3 h after surgery. Significant increases in the ascites volume were observed in the 3.5% NaT (3, 6 and 12 h) and 5% NaT (3, 12 and 48 h) groups compared with those in the NS group (Fig. 1B). Serum amylase levels significantly increased after pancreatic duct perfusion with 3.5% NaT (3, 6, 12 and 24 h) and 5% NaT (3, 6, 12 and 24 h) compared with those in the NS group (Fig. 1C). The amylase levels in ascitic fluid also significantly increased after perfusion with 3.5% NaT (6 and 12 h) and 5% NaT (3, 6, 12 and 24 h), as demonstrated in Fig. 1D. In the 5% NaT group, the serum and ascitic fluid amylase levels exhibited a sustained increase and were maintained at a high level without reduction. No statistically significant difference in amylase levels was observed in the 5% NaT-48 h group. Lipase activity in the 3.5% NaT and 5% NaT groups significantly increased in the serum and ascitic fluid at 3, 6 and 12 h after the infusion and recovered within 24 h (Fig. 1E and F).

Histopathological changes in the pancreas of NaT-induced SAP rats. Histopathological scores were assessed (Table I) according to the levels of pancreatic interstitial edema, leukocyte infiltration, acinar cell necrosis and hemorrhage using H&E staining. Representative images (magnification, x200) of the H&E-stained pancreatic sections are revealed in

Table II. Histopathological findings of lungs tissue.

	Number of case/Total number of each group						
	Alveolar septum thickening area						
Groups	None	≤5%	<20%	≥20%	Leukocyte infiltration	Alveolar capillaries dilation and congestion	Hemorrhage
Sham	5/5	0/5	0/5	0/5	0/5	0/5	0/5
NS	2/5	2/5	1/5	0/5	0/5	0/5	0/5
3.5% NaT							
3 h	1/5	3/5	1/5	0/5	0/5	0/5	0/5
6 h	0/5	0/5	2/5	3/5	1/5	0/5	1/5
12 h	0/5	0/5	2/5	3/5	0/5	0/5	2/5
24 h	0/5	0/5	2/5	3/5	1/5	0/5	0/5
48 h	0/5	0/5	0/5	5/5	2/5	4/5	1/5
72 h	0/4	0/4	1/4	3/4	0/4	2/4	0/4
5% NaT							
3 h	0/5	0/5	1/5	4/5	0/5	0/5	0/5
6 h	0/5	1/5	2/5	2/5	3/5	0/5	1/5
12 h	0/5	2/5	2/5	1/5	2/5	0/5	1/5
24 h	0/5	3/5	0/5	2/5	1/5	0/5	1/5
48 h	0/3	2/3	1/3	0/3	1/3	0/3	0/3

NaT, sodium taurocholate.

Fig. 2. No remarkable difference was observed in the histopathological images of the pancreas between the Sham and NS groups. In the 3.5 and 5% NaT groups, the pancreas was critically damaged in a time- and dose-dependent manner, compared with the NS group. Furthermore, the pancreas in the 5% NaT group exhibited earlier severe acinar cell necrosis, interstitial edema, and hemorrhage compared with that in the 3.5% NaT group (Fig. 2 and Table I). However, leukocyte infiltration was mild in both groups (mostly lymphocytes, plasmacytes, and eosinophils rather than neutrophils).

Proinflammatory cytokines in the serum and ascitic fluid of NaT-induced SAP rats. The protein levels of IL-1β, IL-6, and TNF-α were measured using ELISA to evaluate the inflammatory response in the serum and ascitic fluid of rats with NaT-induced pancreatitis. The levels of IL-1β in ascitic fluid were significantly increased in the 5% NaT-12 h group compared with those in the NS group (P<0.05; Fig. 3D). The levels of IL-6 in ascitic fluid significantly increased in the 5% NaT group at 3, 6 and 12 h, and were alleviated within 48 h (P<0.05 compared with the 12 h group; Fig. 3E). The levels of IL-6 significantly increased in serum at 5% NaT-48 h, Whereas the level of IL-1β and TNF-α in the serum scarcely increased after 3.5 or 5% NaT infusion (Fig. 3A-C). Again, the levels of TNF-α in the serum and ascitic fluid were not elevated (Fig. 3C and F).

Pancreatitis-associated liver and kidney injuries in NaT-induced SAP rats. Compared to the NS group, the AST levels were significantly elevated after infusion in the 3.5% (6 and 12 h) and 5% NaT groups (3, 6 and 12 h; P<0.05; Fig. 3G). The level of ALT in 5% NaT groups (12 h) was significantly increased (P<0.01; Fig. 3H). In 3.5% NaT groups, ALT and AST levels declined back to almost normal levels at 72 h, whereas in the 5% NaT groups a nonsignificant downward trend was observed after 24 h (Fig. 3G and H). Furthermore, the CRE levels increased only in the 5% NaT-3 h group (P<0.01), compared with those in the NS group (Fig. 3I), whereas no statistically significant increase in the serum urea levels was observed (Fig. 3J).

According to the liver histopathology results (Fig. S1), only slight hepatocellular edema and hepatic sinusoid dilation were observed at 12 h (1/3) and 24 h (1/3) in the 5% NaT group. In the kidneys, ~1/3 of the 5% NaT rats at each time point exhibited slight renal tubule edema or renal vascular congestion, and only one rat among all animals developed periglomerular interstitial hemorrhage and ischemic tubular necrosis at 24 h. The most severe pathological findings are shown in Fig. S1. However, changes in the liver and kidneys were considered insufficient for the diagnosis of pathological damage. In addition, no apparent pathological changes in the kidneys and livers were observed in the 3.5% NaT group, even after 72 h (data not shown).

Pancreatitis-associated acute lung injury in NaT-induced SAP rats. Lung sections were stained with H&E and images were obtained (Fig. 4). Histopathological results showed that the 3.5 and 5% NaT groups showed alveolar septum thickening with partial alveolar collapse, alveolar capillary dilation with congestion, or local hemorrhage. Alveolar septum thickening was widely observed in all NaT groups (Table II). Slight neutrophil infiltration was observed in certain cases (Table II). MPO and MDA levels in lung tissue were not significantly increased (Fig. S2).

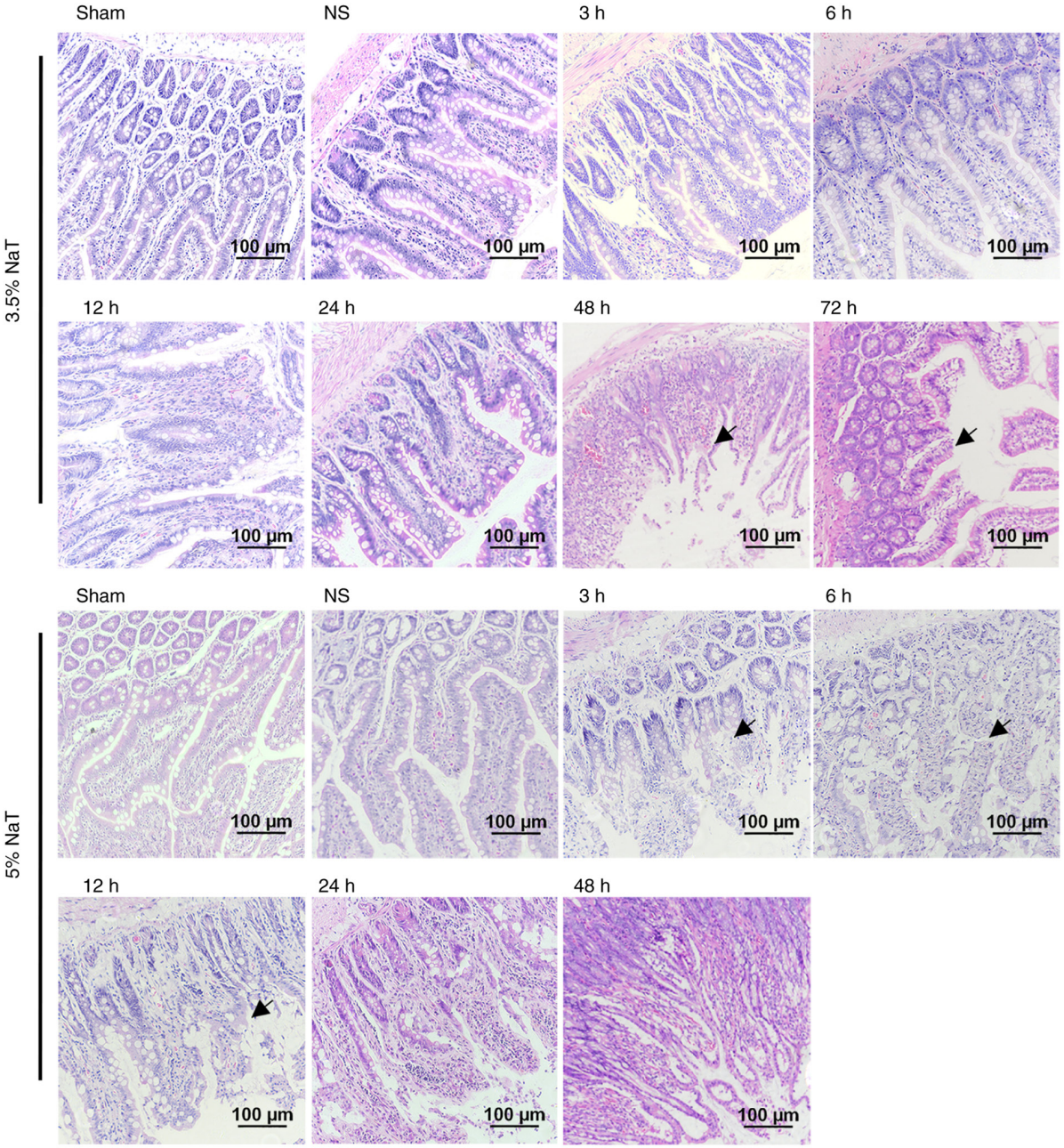

Figure 5. Histopathological changes of the intestinal mucosal in NaT-induced severe acute pancreatitis rats. Representative images of hematoxylin and eosin-stained ileum sections (magnification, x200; scale bar: 100 μm). Normal ileum mucosal histology in the Sham and NS groups; Intestinal villus exfoliation and necrotic areas are pointed with black arrows. NaT, sodium taurocholate; NS, normal saline.

Pancreatitis-associated intestinal mucosal injury in NaT-induced SAP rats. Intestinal mucosal injury was observed in the ileum in the 5% NaT groups using H&E staining (magnification, x200; Fig. 5). In the 5% NaT group, the intestinal mucosal epithelium exhibited abscission, necrosis and hemorrhage at 3 and 6 h after infusion, suggesting that 5% NaT induced mucosal injury in the early stage of SAP. No significant pathological changes in the ileum were observed in the 3.5% NaT group compared with those in the NS group until 48 h (1/3) and 72 h (1/3). Furthermore, immunofluorescence was used to detect alterations in ileal tight junction morphology in the 5% NaT group (24 and 48 h). As expected, disruption of ZO-1 and occludin tight junction constituents was detected in the 5% NaT-48 h group (Fig. 6).

The levels of IL-1β, IL-6 and TNF-α in ileum tissue were detected using ELISA (Fig. S3). The results showed that the IL-1β and TNF-α levels in the 5% NaT group were significantly increased in the ileum at 12 h compared with those in the NS group ($P<0.01$). No statistical difference in the IL-6 levels was observed in either the 3.5 NaT or 5% NaT groups.

Discussion

SAP is a devastating condition characterized by local pancreatitis and systemic complications, commonly originating from biliary (45%) and alcoholic (21%) AP (24). Overall, the mortality rate of patients with SAP may reach 50%, whereas that of all forms of AP is ~2-5% (25). One of the most

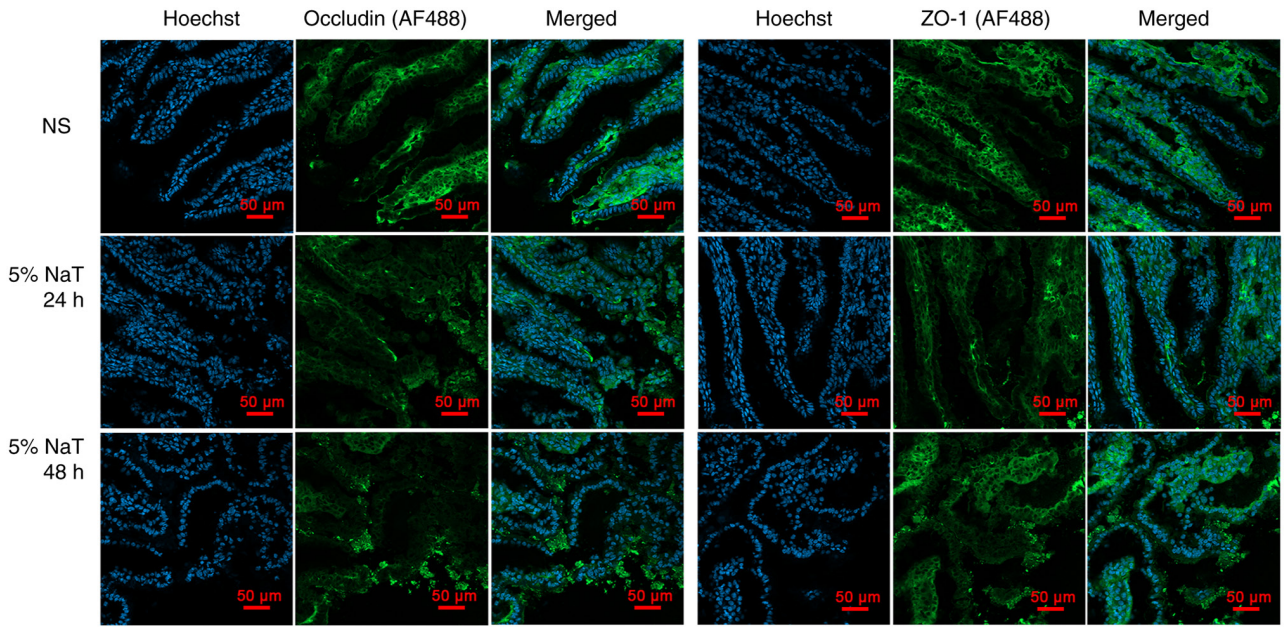

Figure 6. Tight junction proteins of the intestinal mucosa of NaT-induced severe acute pancreatitis rats. Immunofluorescence staining of ileum tissue in rats treated with 5% NaT or NS (scale bar: 50 μm) with antibodies against ZO-1 or occludin. The nuclei are stained with Hoechst. NaT, sodium taurocholate; NS, normal saline; ZO-1, zonula occludens-1.

critical risk factors for mortality in SAP is organ failure (18). However, the mechanisms underlying SAP development remain unclear. To perform a more systematic assessment of organ dysfunction and systemic inflammatory responses in this animal model, multiple organs treated with different NaT concentrations and at different time points were observed and studied.

In the present study, a SAP rat model with two different concentrations of NaT was successfully established and the potential systemic injury in this model was examined. The present results revealed that the ascites volume, amylase and lipase activity in the serum and ascitic fluid significantly increased at both NaT concentrations after infusion, suggesting that our model was successfully established. The mechanism of ascites production is related to the leakage of pancreatic secretions from damaged pancreatic ducts, which occurs when pancreatic secretions accumulate in the peritoneum (26). The severity of ascites production varies widely, often depending on the location and degree of ductal injury and infection in the fluid (26).

In a previous study, the mortality of AP mice that received 4 and 5% taurocholate solutions in the first 24 h was ~10 and 60%, respectively (27). Considering the high mortality rate of this model, the effects of 3.5 and 5% NaT were compared. The histological changes in pancreatic damage in NaT-induced pancreatitis became progressively more severe in all SAP groups during the experiment. The 5% NaT group exhibited earlier and more severe acinar cell necrosis, interstitial edema and hemorrhage than the 3.5% NaT group. However, only mild infiltration of lymphocytes, plasmacytes, and eosinophils, rather than neutrophils, was observed, indicating that pancreatic injury may be considered a hemorrhagic necrotizing injury rather than an inflammatory lesion.

The development of SIRS is an important risk factor for AP (28-30). Therefore, the levels of proinflammatory cytokines, such as IL-1β, Il-6 and TNF-α, were determined. Although it was attempted to monitor the occurrence of SIRS in rats with SAP using cytokine levels, the results were unsatisfactory. Only IL-6 showed a substantial increase in the circulation after 48 h of 5% NaT infusion in the present study, whereas cytokines, such as IL-1β and TNF-α, did not. One possible explanation is that pancreatitis begins with the premature activation of digestive enzymes in pancreatic acinar cells, resulting in cell damage (11,31). This process parallels the infiltration of inflammatory cells and causes organ and pancreatic damage (32). H&E staining of the pancreas revealed more necrosis and hemorrhage in the early stage, while leukocyte infiltration appeared later in this animal model, at 72 h in the 3.5% NaT group, and at 24 and 48 h in the 5% NaT group. Furthermore, intestinal ischemia/reperfusion injuries sustained by pancreatic inflammation may lead to mucosal barrier disruption and bacterial translocation, which may be the first stage in the pathogenesis of sepsis (33,34). Tight junctions between intestinal epithelial cells play an essential role in intestinal permeability. In the present study, ZO-1 and occludin tight junction constituents were disrupted after infusion of 5% NaT for 48 h. This may explain why early stage elevation of serum inflammatory cytokines was minimal. It is hypothesized that this model exhibited a systemic inflammatory response.

Although it was not possible to assess the occurrence of SIRS in terms of serum inflammatory cytokines, a significant release of a large number of inflammatory factors (IL-1β and IL-6) in ascites was observed in the 5% NaT group. Pancreatic ascites results from the leakage of pancreatic secretions into the peritoneum, mostly occurring after a pseudocyst or walled-off necrosis (26). The ascitic fluid contains a large number of lipases, amylase, inflammatory cytokines and necrotic substances, which may cause intra-abdominal hypertension and adhesion of the abdominal organs (35). Symptoms

of SAP can be improved by decreasing the levels of cytokines and abdominal paracentesis drainage has been reported to be beneficial to animals and patients (36-38).

The current clinical diagnosis of SIRS is mainly related to the evaluation of vital signs (body temperature, heart rate and respiration) and leukocyte count, thus lacking specificity (39). Matsumoto *et al* (40) used HMGB1 as a marker of SIRS in rats intraperitoneally injected with cerulein and lipopolysaccharide. However, the serum levels of IL-1β, IL-6, and TNF-α were not measured. Moreover, the activation of NLRP3 is confirmed to regulate the development of SIRS and compensatory anti-inflammatory response syndromes in mice with cerulein-induced AP (37). More sensitive indicators are required to determine the occurrence of SIRS in SAP.

Pancreatic necrosis is associated with poor prognosis, higher mortality and organ failure (41). Multiple organ injury in the SAP rat model was also investigated in the present study. Acute lung injury, acute kidney injury and cardiovascular dysfunction are the most common pancreatitis-associated organ dysfunctions in patients and autopsy findings (19,25). Pancreatitis-associated acute lung injury (12,19), kidney injury (42-44), and liver injury (45) have been reported in experimental models. Clinical findings of respiratory failure (acute respiratory distress syndrome) are correlated with autopsy findings of pleural effusions, acute diffuse alveolar damage and pulmonary congestion (46,47). In the present study, alveolar septum thickening with partial alveolar collapse was widely observed after NaT infusion, representing a possible insufficiency of lung function. Dilation and congestion of alveolar capillaries, which primarily appeared in the 3.5% NaT group at 48 and 72 h, have also been observed in some cases. Neutrophil infiltration was also observed in some cases in our study, but the MPO and MDA levels did not increase in lung tissue.

Shi *et al* (42) reported the features of kidney pathologic injury, such as glomerular degeneration, blurred cell boundaries, tubule epithelial cell swelling and necrosis, interstitial hemorrhage, tubule lumen narrowing, formation of a large number of tubular casts and inflammatory cell infiltration, at 12 h after administration of 5% NaT. However, it was found that even after 5% NaT infusion, most of the animals did not present such pathological changes in the kidneys, whereas only one rat showed periglomerular interstitial hemorrhage and ischemic tubular necrosis in the kidneys after 24 h. Yet, numerous researchers have used this model to investigate drugs related to liver and kidney injury. Occasionally, slight hepatocellular edema and hepatic sinusoid dilation in the liver were observed in the present study; however, these changes may not be sufficient for further efficacy studies. The present results are consistent with those previously reported in a mouse model, in which NaT-induced AP did not show severe kidney and liver pathological damage (27). One possible explanation is that pancreatic necrosis caused by NaT mainly affects the respiratory circulatory system in the early stage, causing a large number of deaths. While the liver adjacent to the pancreas has a strong compensatory capacity, only a transient increase in liver enzymes occurs in the early stage.

Intestinal mucosal ischemia-reperfusion during AP can compromise the integrity of the intestinal barrier and cause intestinal bacterial translocation, resulting in local and systemic infections (48). The gastrointestinal complications of pancreatitis are important and may result in high mortality rates. Bowel complications associated with AP are potentially due to the pancreatic enzymes released to the mesentery, which may result in inflammation, ischemia, necrosis and obstruction of different segments of the intestine (49). Small intestinal mucosal barrier injury may contribute to bacterial translocation and infected pancreatic necrosis, resulting in the pathophysiology of systemic inflammation (19). Intestinal injury has been reported in the NaT-induced SAP model, but most studies have focused on the results obtained at 12, 24 h, or even 24 days after infusion (50-53). In the present study, it was identified that the ileum villi were exfoliated and necrotic in the 5% NaT group, but these injuries were virtually absent in the 3.5% NaT group, indicating that the onset of injury to the intestinal mucosal barrier may occur at the early stage of pancreatitis in this animal model using 5% NaT.

Moreover, local inflammation and intestinal barrier tight junction proteins in ileum tissue were examined. The levels of IL-1β and TNF-α were significantly elevated in the ileum in the 5% NaT-12 h group, and no further increase in the levels of IL-1β, IL-6 and TNF-α was observed after 24 h. According to the pathologist, intestinal mucosal injuries that occurred in the early stage of this animal model are caused by acute ischemic injury rather than bacteria, which is consistent with the finding that the levels of inflammatory factors were not elevated in the early stage. In addition, the expression of the tight junction proteins ZO-1 and occludin was disrupted in the 5% NaT group at 48 h. This result indicated that ischemic injury of the ileum progressed to severe intestinal barrier injury in this model; therefore, there was significant inflammatory infiltration in the intestinal tract or pancreatic necrotic tissue in the 5% NaT group at 48 h.

A likely explanation is that the high mortality in this model is a result of severe pancreatic damage and acute respiratory dysfunction, leading to hemodynamic instability. Unfortunately, indices such as heart rate, blood pressure, blood oxygen saturation, arterial blood gas and other physiological indicators were not included; basic experiments may be helpful in monitoring the severity of AP in rats.

The present study may hopefully provide important information to researchers who intend to carry out animal experiments using NaT-induced SAP models. The present findings will be useful for conducting experiments according to the 3R principles of replacement, reduction, and refinement for the ethical use of animals in research. However, it was also emphasized that there are certain limitations in the application of this model to the study of mechanisms and treatments for pancreatitis-associated acute liver and kidney injuries. Therefore, it is considered that multiple model comparisons are important for efficacy assessment and further mechanistic exploration.

Acknowledgements

Not applicable.

Funding

The present study was supported by the National Natural Science Foundation of China (grant no. 81703859) and the

Health and Family Planning Commission of Shenzhen Municipality (grant no. SZBC2017017).

Availability of data and materials

The datasets used and/or analyzed during the current study are available from the corresponding author on reasonable request.

Authors' contributions

XXH conducted the experiment and wrote the manuscript. HYW designed the study and was involved in revisions. JMY, BFL and YZL carried out the establishment of animal models, including animal feeding and animal surgery. PDH and ZYZ collected and analyzed the data. XXH and JMY confirm the authenticity of all the raw data. QQM and SJG performed part of the experiments and provided professional pathological advice. BH was involved in the design of the study and revised the important intellectual content. YFX contributed to the conception of this study, was involved in the animal surgery and gave final approval of the version to be published. All authors read and approved the final manuscript.

Ethics approval and consent to participate

All animal procedures were conducted according to the Guidelines for Animal Care of Guangzhou University of Chinese Medicine and approved (approval no. ZYD-2020-028) by the Animal Care and Use Committee of Guangzhou University of Chinese Medicine (Guangzhou, China). All efforts were made to minimize the suffering of animals as much as possible.

Patient consent for publication

Not applicable.

Competing interests

The authors declare that they have no competing interests.

References

1. Boxhoorn L, Voermans RP, Bouwense SA, Bruno MJ, Verdonk RC, Boermeester MA, van Santvoort HC and Besselink MG: Acute pancreatitis. Lancet 396: 726-734, 2020.
2. Xiao AY, Tan ML, Wu LM, Asrani VM, Windsor JA, Yadav D and Petrov MS: Global incidence and mortality of pancreatic diseases: A systematic review, meta-analysis, and meta-regression of population-based cohort studies. Lancet Gastroenterol Hepatol 1: 45-55, 2016.
3. Schepers NJ, Bakker OJ, Besselink MG, Ahmed Ali U, Bollen TL, Gooszen HG, van Santvoort HC and Bruno MJ; Dutch Pancreatitis Study Group: Impact of characteristics of organ failure and infected necrosis on mortality in necrotising pancreatitis. Gut 68: 1044-1051, 2019.
4. van Santvoort HC, Bakker OJ, Bollen TL, Besselink MG, Ahmed Ali U, Schrijver AM, Boermeester MA, van Goor H, Dejong CH, van Eijck CH, *et al*: A conservative and minimally invasive approach to necrotizing pancreatitis improves outcome. Gastroenterology 141: 1254-1263, 2011.
5. Bang JY, Wilcox CM, Arnoletti JP and Varadarajulu S: Superiority of endoscopic interventions over minimally invasive surgery for infected necrotizing pancreatitis: Meta-analysis of randomized trials. Dig Endosc 32: 298-308, 2020.
6. Banks PA, Bollen TL, Dervenis C, Gooszen HG, Johnson CD, Sarr MG, Tsiotos GG and Vege SS; Acute Pancreatitis Classification Working Group: Classification of acute pancreatitis-2012: Revision of the Atlanta classification and definitions by international consensus. Gut 62: 102-111, 2013.
7. Moggia E, Koti R, Belgaumkar AP, Fazio F, Pereira SP, Davidson BR and Gurusamy KS: Pharmacological interventions for acute pancreatitis. Cochrane Database Syst Rev 4: CD011384, 2017.
8. Aho HJ and Nevalainen TJ: Experimental pancreatitis in the rat. Ultrastructure of sodium taurocholate-induced pancreatic lesions. Scand J Gastroenterol 15: 417-424, 1980.
9. Aho HJ, Koskensalo SM and Nevalainen TJ: Experimental pancreatitis in the rat. Sodium taurocholate-induced acute haemorrhagic pancreatitis. Scand J Gastroenterol 15: 411-416, 1980.
10. Laukkarinen JM, Van Acker GJ, Weiss ER, Steer ML and Perides G: A mouse model of acute biliary pancreatitis induced by retrograde pancreatic duct infusion of Na-taurocholate. Gut 56: 1590-1598, 2007.
11. Saluja A, Dudeja V, Dawra R and Sah RP: Early intra-acinar events in pathogenesis of pancreatitis. Gastroenterology 156: 1979-1993, 2019.
12. Su KH, Cuthbertson C and Christophi C: Review of experimental animal models of acute pancreatitis. HPB (Oxford) 8: 264-286, 2006.
13. Serra MB, Koike MK, Barbeiro DF, Machado MCC and de Souza HP: Sodium taurocholate induced severe acute pancreatitis in C57BL/6 Mice. J Vis Exp 172: e61547, 2021.
14. Yang X, Geng H, You L, Yuan L, Meng J, Ma Y, Gu X and Lei M: Rhein protects against severe acute pancreatitis in vitro and in vivo by regulating the JAK2/STAT3 pathway. Front Pharmacol 13: 778221, 2022.
15. Liu ZH, Peng JS, Li CJ, Yang ZL, Xiang J, Song H, Wu XB, Chen JR and Diao DC: A simple taurocholate-induced model of severe acute pancreatitis in rats. World J Gastroenterol 15: 5732-5739, 2009.
16. Guo P, Liu L, Yang X, Li M, Zhao Q and Wu H: Irisin improves BBB dysfunction in SAP rats by inhibiting MMP-9 via the ERK/NF-κB signaling pathway. Cell Signal 93: 110300, 2022.
17. Qi H, Lu Q, Yin C, Xiao H, Wen Y, Zhang S, Cui Q and Yang W: Exogenous leptin protects rat models of sodium taurocholate-induced severe acute pancreatitis through endocrinal and immunological pathways. Mol Med Rep 16: 6306-6312, 2017.
18. Guo Q, Li A, Xia Q, Liu X, Tian B, Mai G, Huang Z, Chen G, Tang W, Jin X, *et al*: The role of organ failure and infection in necrotizing pancreatitis: A prospective study. Ann Surg 259: 1201-1207, 2014.
19. Garg PK and Singh VP: Organ failure due to systemic injury in acute pancreatitis. Gastroenterology 156: 2008-2023, 2019.
20. Johnson CD and Abu-Hilal M: Persistent organ failure during the first week as a marker of fatal outcome in acute pancreatitis. Gut 53: 1340-1344, 2004.
21. Mofidi R, Duff MD, Wigmore SJ, Madhavan KK, Garden OJ and Parks RW: Association between early systemic inflammatory response, severity of multiorgan dysfunction and death in acute pancreatitis. Br J Surg 93: 738-744, 2006.
22. Mowbray NG, Ben-Ismaeil B, Hammoda M, Shingler G and Al-Sarireh B: The microbiology of infected pancreatic necrosis. Hepatobiliary Pancreat Dis Int 17: 456-460, 2018.
23. Schmidt J, Rattner DW, Lewandrowski K, Compton CC, Mandavilli U, Knoefel WT and Warshaw AL: A better model of acute pancreatitis for evaluating therapy. Ann Surg 215: 44-56, 1992.
24. Matta B, Gougol A, Gao X, Reddy N, Talukdar R, Kochhar R, Goenka MK, Gulla A, Gonzalez JA, Singh VK, *et al*: Worldwide variations in demographics, management, and outcomes of acute pancreatitis. Clin Gastroenterol Hepatol 18: 1567-1575.e2, 2020.
25. Gliem N, Ammer-Herrmenau C, Ellenrieder V and Neesse A: Management of severe acute pancreatitis: An update. Digestion 102: 503-507, 2021.
26. Gapp J, Hoilat GJ and Chandra S: Pancreatic ascites. In: StatPearls. Treasure Island (FL): StatPearls Publishing, 2020.
27. Wittel UA, Wiech T, Chakraborty S, Boss B, Lauch R, Batra SK and Hopt UT: Taurocholate-induced pancreatitis: A model of severe necrotizing pancreatitis in mice. Pancreas 36: e9-e21, 2008.
28. Malmstrøm ML, Hansen MB, Andersen AM, Ersbøll AK, Nielsen OH, Jørgensen LN and Novovic S: Cytokines and organ failure in acute pancreatitis: Inflammatory response in acute pancreatitis. Pancreas 41: 271-277, 2012.

29. Hirota M, Nozawa F, Okabe A, Shibata M, Beppu T, Shimada S, Egami H, Yamaguchi Y, Ikei S, Okajima T, *et al*: Relationship between plasma cytokine concentration and multiple organ failure in patients with acute pancreatitis. Pancreas 21: 141-146, 2000.
30. Brivet FG, Emilie D and Galanaud P: Pro- and anti-inflammatory cytokines during acute severe pancreatitis: An early and sustained response, although unpredictable of death. Parisian study group on acute pancreatitis. Crit Care Med 27: 749-755, 1999.
31. Sendler M, Maertin S, John D, Persike M, Weiss FU, Krüger B, Wartmann T, Wagh P, Halangk W, Schaschke N, *et al*: Cathepsin B activity initiates apoptosis via digestive protease activation in pancreatic acinar cells and experimental pancreatitis. J Biol Chem 291: 14717-14731, 2016.
32. Sendler M, Weiss FU, Golchert J, Homuth G, van den Brandt C, Mahajan UM, Partecke LI, Döring P, Gukovsky I, Gukovskaya AS, *et al*: Cathepsin B-mediated activation of trypsinogen in endocytosing macrophages increases severity of pancreatitis in mice. Gastroenterology 154: 704-718.e10, 2018.
33. Zhang J, Yu WQ, Wei T, Zhang C, Wen L, Chen Q, Chen W, Qiu JY, Zhang Y and Liang TB: Effects of short-peptide-based enteral nutrition on the intestinal microcirculation and mucosal barrier in mice with severe acute pancreatitis. Mol Nutr Food Res 64: e1901191, 2020.
34. de Madaria E, Martínez J, Lozano B, Sempere L, Benlloch S, Such J, Uceda F, Francés R and Pérez-Mateo M: Detection and identification of bacterial DNA in serum from patients with acute pancreatitis. Gut 54: 1293-1297, 2005.
35. ShaykhoIslami A, Ghasemian M, Zardast M and Farzad M: Effect of intra-abdominal administration of ascites fluid on postoperative peritoneal adhesion in rat model: A randomized controlled trail. Ann Med Surg (Lond) 71: 102928, 2021.
36. Baroja-Mazo A, Martín-Sánchez F, Gomez AI, Martínez CM, Amores-Iniesta J, Compan V, Barberà-Cremades M, Yagüe J, Ruiz-Ortiz E, Antón J, *et al*: The NLRP3 inflammasome is released as a particulate danger signal that amplifies the inflammatory response. Nat Immunol 15: 738-748, 2014.
37. Sendler M, van den Brandt C, Glaubitz J, Wilden A, Golchert J, Weiss FU, Homuth G, De Freitas Chama LL, Mishra N, Mahajan UM, *et al*: NLRP3 inflammasome regulates development of systemic inflammatory response and compensatory anti-inflammatory response syndromes in mice with acute pancreatitis. Gastroenterology 158: 253-269.e14, 2020.
38. Liu RH, Wen Y, Sun HY, Liu CY, Zhang YF, Yang Y, Huang QL, Tang JJ, Huang CC and Tang LJ: Abdominal paracentesis drainage ameliorates severe acute pancreatitis in rats by regulating the polarization of peritoneal macrophages. World J Gastroenterol 24: 5131-5143, 2018.
39. Kaukonen KM, Bailey M, Pilcher D, Cooper DJ and Bellomo R: Systemic inflammatory response syndrome criteria in defining severe sepsis. N Engl J Med 372: 1629-1638, 2015.
40. Matsumoto M, Kamei K, Chikugo T, Matsumoto I, Kawaguchi K and Takeyama Y: Efficacy of recombinant human-soluble thrombomodulin for severe acute pancreatitis in a rat experimental model. Pancreas 49: 503-508, 2020.
41. Rashid MU, Hussain I, Jehanzeb S, Ullah W, Ali S, Jain AG, Khetpal N and Ahmad S: Pancreatic necrosis: Complications and changing trend of treatment. World J Gastrointest Surg 11: 198-217, 2019.
42. Shi Q, Liao KS, Zhao KL, Wang WX, Zuo T, Deng WH, Chen C, Yu J, Guo WY, He XB, *et al*: Hydrogen-rich saline attenuates acute renal injury in sodium taurocholate-induced severe acute pancreatitis by inhibiting ROS and NF-κB pathway. Mediators Inflamm 2015: 685043, 2015.
43. Zhu S, Zhang C, Weng Q and Ye B: Curcumin protects against acute renal injury by suppressing JAK2/STAT3 pathway in severe acute pancreatitis in rats. Exp Ther Med 14: 1669-1674, 2017.
44. Zhang XH, Li ML, Wang B, Guo MX and Zhu RM: Caspase-1 inhibition alleviates acute renal injury in rats with severe acute pancreatitis. World J Gastroenterol 20: 10457-10463, 2014.
45. Li YY, Li XL, Yang CX, Zhong H, Yao H and Zhu L: Effects of tetrandrine and QYT on ICAM-1 and SOD gene expression in pancreas and liver of rats with acute pancreatitis. World J Gastroenterol 9: 155-159, 2003.
46. Stoppacher R: Sudden death due to acute pancreatitis. Acad Forensic Pathol 8: 239-255, 2018.
47. Yang A, Zhang L and Vege SS: Autopsy study of patients dying due to acute pancreatitis: 262. Am Coll Gastroenterol 109: S81, 2014.
48. Li XY, He C, Zhu Y and Lu NH: Role of gut microbiota on intestinal barrier function in acute pancreatitis. World J Gastroenterol 26: 2187-2193, 2020.
49. Bansal A, Gupta P, Singh H, Samanta J, Mandavdhare H, Sharma V, Sinha SK, Dutta U and Kochhar R: Gastrointestinal complications in acute and chronic pancreatitis. JGH Open 3: 450-455, 2019.
50. Piao X, Liu B, Sui X, Niu W, Zhang Q, Shi X, Cai S and Fan Y: Picroside II improves severe acute pancreatitis-induced intestinal barrier injury by inactivating oxidative and inflammatory TLR4-dependent PI3K/AKT/NF-κB signaling and improving gut microbiota. Oxid Med Cell Longev 2020: 3589497, 2020.
51. Su S, Liang T, Zhou X, He K, Li B and Xia X: Qingyi decoction attenuates severe acute pancreatitis in rats via inhibition of inflammation and protection of the intestinal barrier. J Int Med Res 47: 2215-2227, 2019.
52. Ye J, Dai H, Liu Y, Yu B, Yang J and Fei A: Blockade of C3a/C3aR axis alleviates severe acute pancreatitis-induced intestinal barrier injury. Am J Transl Res 12: 6290-6301, 2020.
53. Ning JW, Zhang Y, Yu MS, Gu ML, Xu J, Usman A and Ji F: Emodin alleviates intestinal mucosal injury in rats with severe acute pancreatitis via the caspase-1 inhibition. Hepatobiliary Pancreat Dis Int 16: 431-436, 2017.